Bioconjugate Chemistry

pubs.acs.org/bc

Communication

Influence of Riboflavin Targeting on Tumor Accumulation and Internalization of Peptostar Based Drug Delivery Systems

Milita Darguzyte,[#] Regina Holm,[#] Jasmin Baier, Natascha Drude, Jennifer Schultze, Kaloian Koynov, David Schwiertz, Seyed Mohammadali Dadfar, Twan Lammers, Matthias Barz,* and Fabian Kiessling*

Cite This: *Bioconjugate Chem.* 2020, 31, 2691−2696

Read Online

ACCESS | Metrics & More | Article Recommendations | Supporting Information

ABSTRACT: Riboflavin carrier protein (RCP) and riboflavin transporters (RFVTs) have been reported to be highly overexpressed in various cancer cells. Hence, targeting RCP and RFVTs using riboflavin may enhance tumor accumulation and internalization of drug delivery systems. To test this hypothesis, butyl-based 3-arm peptostar polymers were synthesized consisting of a lysine core (10 units per arm) and a sarcosine shell (100 units per arm). The end groups of the arms and the core were successfully modified with riboflavin and the Cy5.5 fluorescent dye, respectively. While in phosphate buffered saline the functionalized peptostars showed a bimodal behavior and formed supramolecular structures over time, they were stable in the serum maintaining their hydrodynamic diameter of 12 nm. Moreover, the polymers were biocompatible and the uptake of riboflavin targeted peptostars in A431 and PC3 cells was higher than in nontargeted controls and could be blocked competitively. In vivo, the polymers showed a moderate passive tumor accumulation, which was not significantly different between targeted and nontargeted peptostars. Nonetheless, at the histological level, internalization into tumor cells was strongly enhanced for the riboflavin-targeted peptostars. Based on these results, we conclude that passive accumulation is dominating the accumulation of peptostars, while tumor cell internalization is strongly promoted by riboflavin targeting.

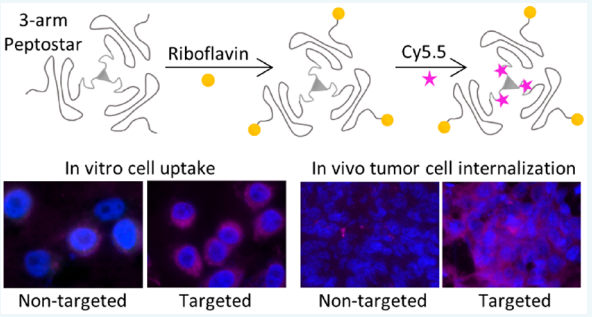

Cancer is a major reason for death worldwide. It is estimated that cancer caused 9.6 million deaths in 2018, and curative treatments of advanced stages are not available for many tumor types.[1] Currently, the best treatment options are surgery, radiotherapy, and chemotherapy. Unfortunately, surgery and radiotherapy are not always possible due to the location of the tumor or the presence of multiple metastases. Thus, chemotherapy is often the only available option to treat advanced tumor stages. Due to their nonspecific accumulation, chemotherapeutics cause damage not only to tumors but also to vital tissues.[2] One option to reduce the nonspecific accumulation of chemotherapeutics is the use of nanosized drug delivery systems.[3] These systems passively accumulate in the tumors due to the enhanced permeability and retention (EPR) effect.[4] In order to further improve drug targeting, the delivery systems can be functionalized to actively target tumor cells or the tumor microenvironment. Here, vitamin receptors that are overexpressed in many cancers are promising targets. Mainly folate[5] and biotin[6] receptors have been evaluated so far, but there are other vitamins that are highly expressed at tumor sites and not yet explored in greater detail.

Vitamin B2, Riboflavin (RF), is responsible for normal cellular metabolism, proliferation, and growth. It also exhibits antioxidant and anti-inflammatory properties.[7,8] Mammals are not able to synthesize RF; thus, it must be acquired from their diet. Absorbed RF is distributed to different tissue compartments via the circulation, and the vitamin is transported into cells across the plasma membrane by specialized carrier-mediated processes. These RF transporters were recently identified and classified as RFVT1, RFVT2, and RFVT3.[9] RFVTs and the RF carrier protein have been shown to be highly expressed in breast,[10−14] prostate,[15] liver,[16] esophageal,[17,18] and brain[19] cancers, as well as in squamous cell carcinoma.[14] This makes RF a promising ligand for active targeting of drugs and drug delivery systems.[20]

Like poly(ethylene glycol) (PEG), polysarcosine (pSar) is a protein-resistant material that can introduce stealth-like properties to a surface at high grafting densities.[21−24] Polypept(o)ide stars (a.k.a. peptostars) are consisting of polysarcosine and polypeptide-based polymers.[25−27] These star-like polymers can be synthesized with precise control over the size of the functional core and the respective corona by simply adjusting the degree of polymerization. Besides the functionalization of the end groups of the stars, the core can be

Received: November 2, 2020
Revised: November 23, 2020
Published: November 25, 2020

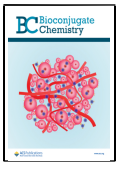

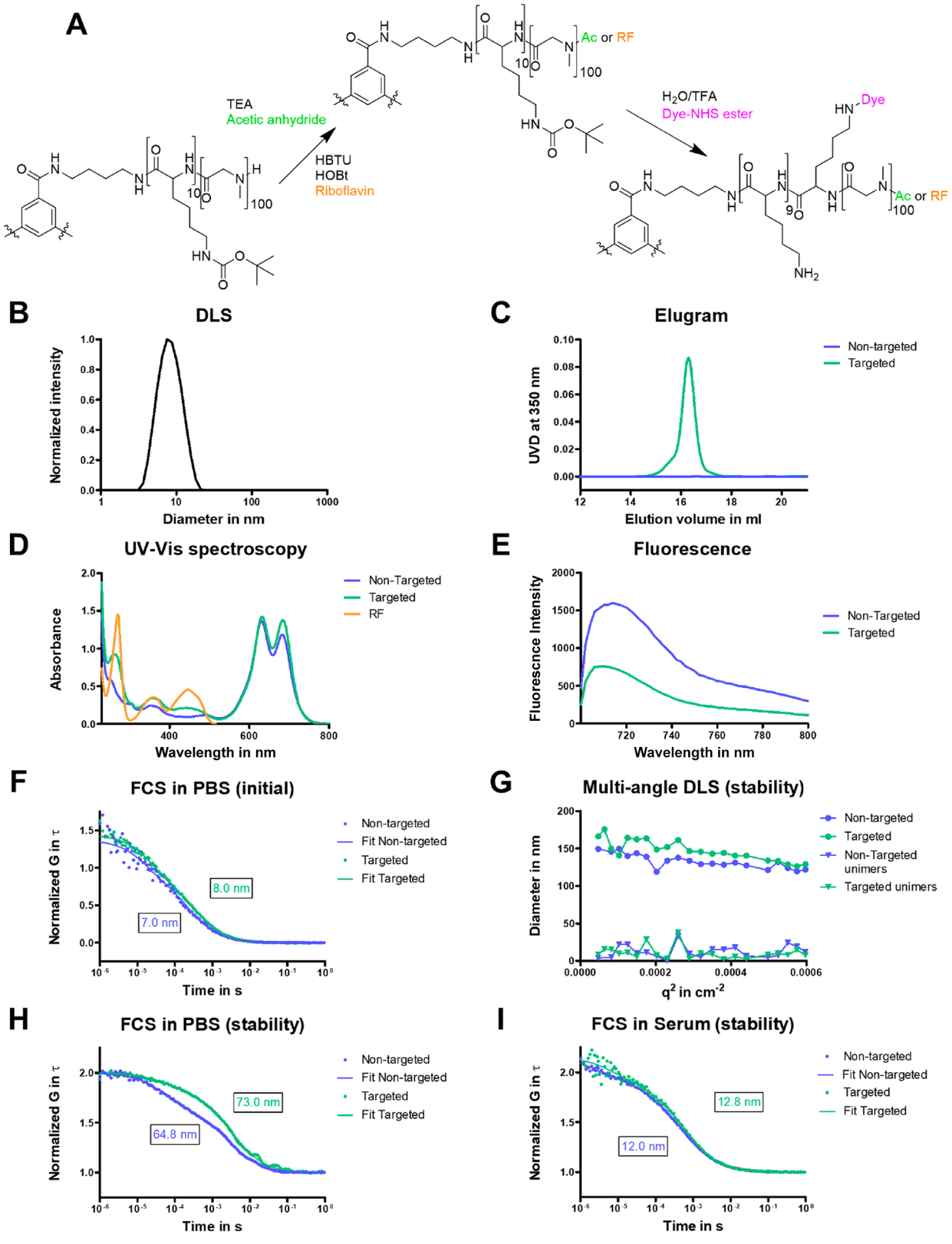

Figure 1. Peptostar characterization: (A) Peptostar functionalization scheme. (B) DLS measurements in methanol of nonfunctionalized nonfluorescent peptostars. (C) SEC elugram at 350 nm. Targeted peptostars show a peak confirming RF conjugation. (D) UV−vis spectroscopy in PBS. Targeted and nontargeted peptostars show absorbance peaks at 633 and 685 nm proving that the labeling with the dye was successful. Additionally, riboflavin peaks at 260 and 460 nm indicate its presence on targeted peptostars. (E) Fluorescence intensity measurements of peptostars excited at 680 nm. Nontargeted peptostars show higher fluorescence compared to targeted ones. (F) FCS measurement in PBS after functionalization. (G–I) Stability measurements of peptostars synthesized more than 3 months ago: (G) multiangle DLS measurements in PBS; (H) FCS measurements in PBS; (I) FCS measurements in serum.

https://dx.doi.org/10.1021/acs.bioconjchem.0c00593
Bioconjugate Chem. 2020, 31, 2691−2696

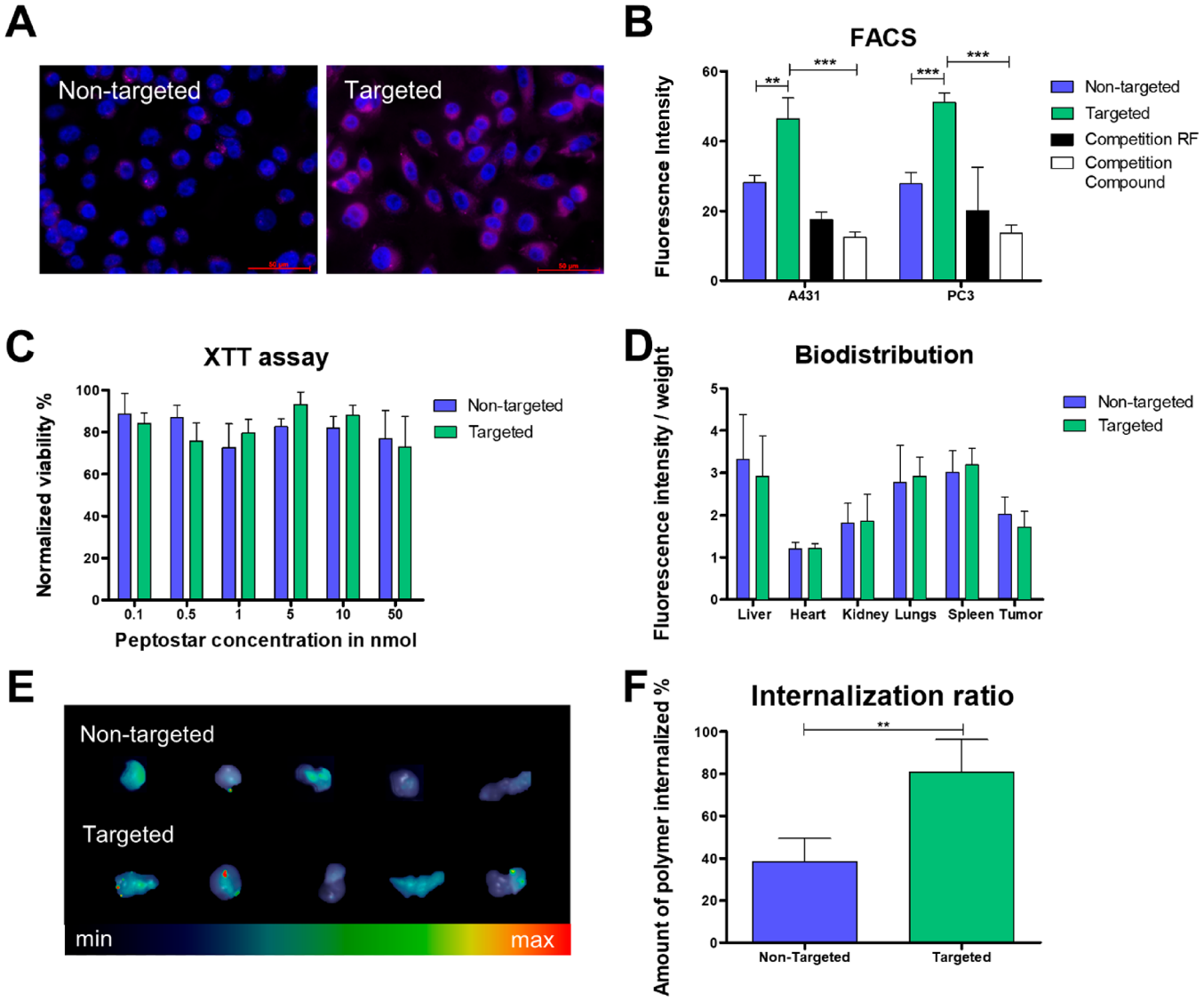

Figure 2. In vitro and ex vivo results: (A) Fluorescence microscopy images of PC3 cells after incubation with polymers (purple) are in line with the quantification and show higher uptake of targeted peptostars. Cell nuclei are stained in blue with DAPI. Scale bar indicates 50 μm. (B) Quantification of cellular uptake of peptostars by A431 and PC3 cells based on FACS. The measurements show a higher uptake of targeted versus nontargeted polymers and a reduction of cellular internalization after blocking the RF receptors. (C) XTT assay of NIH cells after 24 h exposure to polymers. (D) Biodistribution of peptostars inside selected organs and tumor. The total fluorescence intensity is normalized according to the weight of the tissue. No difference can be seen between targeted and nontargeted peptostar biodistribution. (E) 2D FRI images of tumors. Targeted and nontargeted peptostars have similar tumor accumulation. (F) Total tumor accumulation vs intracellular accumulation of peptostars. The targeted peptostars show higher internalization compared to control ones.

labeled, for example, with a fluorescent dye or a chemotherapeutic agent. Hence, peptostars can be functionalized to have both therapeutic and diagnostic (theranostic) properties. Therefore, polypept(o)ide stars, based on polylysine and polysarcosine, are suitable for the functionalization with RF and, thus, allow for analysis of active versus passive targeting.

In this study, butyl-based 3-arm polypept(o)ide stars were synthesized with a protected polylysine core of in total 30 lysine units and a polysarcosine corona of 300 units as described previously.[26,27] In detail, a butyl-based 3-arm initiator was synthesized and used for the controlled ring-opening polymerization of the Lys(Boc)N-Carboxyanhydride (NCA) at first and afterward of the SarNCA. The block lengths of each arm can be precisely adjusted by the monomer to initiator ratio. The synthesized peptostar revealed a low dispersity index of 1.14, as indicated by hexafluoroisopropanol (HFIP) size exclusion chromatography (SEC), and showed a hydrodynamic diameter of 7.6 nm with a polydispersity index (PDI) of 0.16 according to single-angle dynamic light scattering (DLS) measurements in methanol (Figure 1B).

After the synthesis of star-like polymers, the N-termini of the peptostars were functionalized with RF via peptide bond formation or capped by acetylation (Figure 1A). The successful functionalization was determined via nuclear magnetic resonance (NMR) spectroscopy and SEC. The SEC elugram at a wavelength of 350 nm displayed a peak for RF functionalized peptostars, while acetylated ones did not show any signal (Figure 1C). For the dye attachment, first, the Boc group was removed under acidic conditions and then Cy5.5 dye was conjugated via NHS ester linkage (Figure 1A). The successful dye conjugation was confirmed by UV−vis spectroscopy (Figure 1D). The absorbance peaks at 633 and

https://dx.doi.org/10.1021/acs.bioconjchem.0c00593
Bioconjugate Chem. 2020, 31, 2691−2696

685 nm indicated the presence of the dye. Additionally, peaks at 260 and 460 nm were seen for RF functionalized peptostars. Fluorescence properties of peptostars were assessed using a spectrophotometer. At the same concentration, control peptostars showed higher fluorescence than the targeted ones (Figure 1E). It is possible that nontargeted peptostars have more dye molecules attached to their core than functionalized ones. Additionally, RF is known to quench certain fluorescent dyes.[28] Since the labeling procedure for both polymers was the same, it seems more likely that RF quenches Cy5.5. Thus, for further experiments concentrations were chosen according to the equal fluorescence of both samples.

After the functionalization, fluorescence correlation spectroscopy (FCS) measurements in phosphate buffered saline (PBS) were performed. The results showed that control peptostars had a 7.0 nm hydrodynamic diameter, while functionalized ones had 8.0 nm (Figure 1F). Furthermore, to check the dispersion stability, multiangle DLS (ALV/CGS-3, Germany) measurements using peptostars synthesized more than 3 months ago were performed. The solutions demonstrated bimodality: small unimers and big, possibly, supramolecular structures were found (Figure 1G). The unimer size varied according to the angle on average being 11 ± 8 nm for targeted peptostars and 12 ± 8 nm for control ones. The size dependence on an angle indicates that these structures have nonspherical shape. Additionally, we found the larger structures to have an average hydrodynamic diameter of 148 ± 14 nm for targeted and 132 ± 9 nm for nontargeted polymers. We presume these structures to be micelle-like as their size did not significantly vary according to an angle. Taking into consideration that micelles are formed only when the polymer concentration is above critical micelle concentration (CMC), we suspect that at lower concentrations such as used for FCS measurements the peptostars would not form these supramolecular structures. To check this hypothesis, the samples were diluted and measured using FCS. As expected, the structures of approximately 140 nm size were not seen; instead, peptostars formed smaller clusters that had a hydrodynamic diameter of 73.0 nm for targeted and 64.8 nm for nontargeted polymers (Figure 1H). It is noteworthy that the unimers were also not seen as the sample appeared to be uniform. Hence, we assume that the change in concentration destabilized the colloidal dispersion and caused the polymers to redistribute. This implies that the aggregations are concentration-dependent and not based on chemical interactions. Furthermore, to mimic in vivo environments, the polymers were dissolved in the serum and size was measured using FCS. In the serum, nontargeted peptostars had a hydrodynamic diameter of 12.0 nm, while targeted ones measured 12.8 nm (Figure 1I). The slight increase in the size compared to initial FCS measurements in PBS (Figure 1F) could be a result of polymer interaction with the proteins in the serum. Based on these results, we suspect that peptostars tend to form aggregates only in PBS but are stable in serum. Cy5.5 is known to be hydrophobic; thus, if exposed to water, it tends to aggregate. Hence, it is assumed that Cy5.5 inside the core of the peptostar was not sufficiently shielded by the three polysarcosine arms and thus rendered the systems more amphiphilic. On the other hand, this was not the case when peptostars were dissolved in the serum. It is assumed that the proteins that are present in the serum interfered with the peptostars, shielded their hydrophobic core, and as a consequence prevented the formation of larger structures. Similar behavior is known for other amphiphilic substances such as the contrast agent Gadofluorine, which forms micelles only in PBS but is stabilized and kept in the blood circulation by protein interactions in vivo.[29] We postulate that in vitro and in vivo peptostars should behave similarly to those in the serum.

In a previous study, the toxicity of nonfunctionalized, nonfluorescent peptostars was tested on human cervical epithelial carcinoma (HeLa), human embryonic kidney (HEK 293), and mouse dendritic (DC 2.4) cells using the CellTiter-Glo Luminescent cell viability assay.[26] Only a minor decrease in cell viability was seen using concentrations up to 1 mg/mL. In line with these results, we observed no toxic effects for our RF functionalized and control nonfluorescent peptostars that were tested on mouse fibroblast (NIH) cells using XTT colorimetric cell viability assay, in concentrations up to 1.5 mg/mL (Figure 2C). To assess the cellular uptake of peptostars with and without RF, squamous cell carcinoma (A431) and prostate cancer (PC3) cell lines were chosen. Both cell lines have been shown to overexpress RFVTs.[14,15] Polymer internalization was initially evaluated using fluorescence microscopy (Figure 2A). The results were further confirmed by flow cytometry (FACS). In both cell lines, the uptake of targeted peptostars was superior to that of nontargeted ones (Figure 2B). Competitive binding experiments with either preexposure of the cells to 10-fold higher dose of free RF or nonfluorescent targeted peptostars showed significant ($p < 0.001$) reductions in targeted peptostar uptake. These results are in line with the hypothesis that RF-functionalized peptostars are taken up via a transporter-mediated pathway. Furthermore, these results are in agreement with two previous studies in which liposomes[30] and 4-arm PEGs[31] were investigated as RF-targeted systems.

Biodistribution experiments were carried out on Balb/c nude mice bearing A431 xenografts. Peptostars were injected into the tail vein, and after 30 min, the mice were sacrificed, and organs of interest and tumors were dissected and imaged using 2D fluorescence reflectance imaging (FMT2500, PerkinElmer). The 30 min time point was chosen because no long circulation times are expected for the small peptostars, the sizes of which are at the renal elimination threshold. Furthermore, the benefit of active targeting is usually prominent at early time points, especially since RF uptake is known to be a very fast process,[14] while passive accumulation dominates at later time points. By visual inspection of ex vivo images, the highest fluorescence is seen in the liver and kidneys (Figure S1). Since the tumors were smaller than other organs, the fluorescence intensity signals were normalized according to the tissue weight (Table S1). The quantification revealed the highest fluorescence per gram of tissue in the liver, lungs, and spleen (Figure 2D). We postulate that high lung, liver, and spleen accumulation is due to uptake by cells of the mononuclear phagocyte system (MPS). In this context, please note that, due to the thickness and strong optical absorption of liver and spleen tissue, the peptostar accumulation may be underestimated in comparison to other organs. The fluorescence signal in the kidneys points to partial renal excretion of the peptostars. In line with this, lower fluorescence signal in the heart compared to the other organs indicate that most of the polymer is already cleared 30 min post-injection. Therefore, we do not expect major changes in the biodistribution after this time point.

https://dx.doi.org/10.1021/acs.bioconjchem.0c00593
Bioconjugate Chem. 2020, 31, 2691−2696

No difference in tumor accumulation of targeted and control peptostars could be seen (Figure 2E), which is in line with results from the comparison of nontargeted and RF-targeted 4-arm PEG polymers of 13 nm diameter.[31] However, in this study RF-targeting of 4-arm PEG did enhance tumor cell internalization. To test if this was also the case for 3-arm peptostars, tumors were further analyzed histologically. Fluorescence images of fresh cryosections were taken to assess the whole accumulated polymer content, while for the quantification of the internalized content, the cryosections were extensively washed before imaging. Around 80% of targeted peptostars were internalized, which was significantly ($p < 0.01$) more than nontargeted ones (38%) (Figure 2F). This points to a successful tumor cell targeting of our system.

In conclusion, like other polysarcosine systems, 3-arm peptostars with pLys core are biocompatible and do not show cytotoxicity up to 1 mg/mL. Labeling these systems with Cy5.5 at the core increased their tendency to form aggregates in PBS, while in the serum, the polymers interacted with the proteins and had only a slight increase in size. Choosing more hydrophilic imaging tags like radiometal-containing chelate complexes, which would be preferable for clinical translation, may solve this issue. Alternatively, generating peptostars with a higher number of arms should improve the shielding of their core. This would be a preferred solution, since in the future, the imaging tag will be replaced by a hydrophobic chemotherapeutic. In this context, we could already show improved stability of 6-arm versus 3-arm peptostars with a glutamic acid core in PBS and serum.[25] Though our systems had a different core, we assume that the effect of more arms will be similar. From in vivo experiments, it was seen that the circulation time of peptostars was short, as the blood concentration was very low 30 min post-injection. Interestingly, despite the lacking difference in tumor accumulation, RF-targeted 3-arm peptostars did show improved internalization compared to control polymers. Hence, tumor accumulation does not necessarily mean tumor cell internalization, and active targeting using RF is beneficial as it enhances the internalization. For a drug delivery system, this results in a higher drug load being taken up by the cancer cells instead of being released in the tumor interstitial space where it is likely to be taken up by the macrophages. Nonetheless, macrophage internalization does not always lead to reduced drug efficiency, as these cells can work as reservoirs and release drugs slowly to the cancer cells.[32] However, this only holds true for drugs capable of passively entering cancer cells after interstitial release. Furthermore, except for drugs targeting the tumor stroma or immune cells, in the end, only the drug content internalized by cancer cells is responsible for the tumor eradication, and thus, the increased probe internalization by cancer cells due to RF-targeting could result in significantly enhanced antitumor activity even if it is only improved by a factor of 2. However, proving this hypothesis using drug-loaded peptostar systems with longer blood half-life is still open and will be the aim of our future studies.

■ ASSOCIATED CONTENT

Supporting Information

The Supporting Information is available free of charge at https://pubs.acs.org/doi/10.1021/acs.bioconjchem.0c00593.

Materials and methods, including Figure S1 and Table S1 (PDF)

■ AUTHOR INFORMATION

Corresponding Authors

Matthias Barz − *Institute for Organic Chemistry, Johannes Gutenberg-University Mainz, 55128 Mainz, Germany;* orcid.org/0000-0002-1749-9034; Email: barz@uni-mainz.de

Fabian Kiessling − *Institute for Experimental Molecular Imaging, University Hospital Aachen, 52074 Aachen, Germany; Fraunhofer MEVIS, Institute for Medical Image Computing, 52074 Aachen, Germany;* orcid.org/0000-0002-7341-0399; Email: fkiessling@ukaachen.de

Authors

Milita Darguzyte − *Institute for Experimental Molecular Imaging, University Hospital Aachen, 52074 Aachen, Germany*

Regina Holm − *Institute for Organic Chemistry, Johannes Gutenberg-University Mainz, 55128 Mainz, Germany*

Jasmin Baier − *Institute for Experimental Molecular Imaging, University Hospital Aachen, 52074 Aachen, Germany*

Natascha Drude − *Institute for Experimental Molecular Imaging, University Hospital Aachen, 52074 Aachen, Germany*

Jennifer Schultze − *Max Planck Institute for Polymer Research, 55128 Mainz, Germany*

Kaloian Koynov − *Max Planck Institute for Polymer Research, 55128 Mainz, Germany;* orcid.org/0000-0002-4062-8834

David Schwiertz − *Institute for Organic Chemistry, Johannes Gutenberg-University Mainz, 55128 Mainz, Germany*

Seyed Mohammadali Dadfar − *Institute for Experimental Molecular Imaging, University Hospital Aachen, 52074 Aachen, Germany;* orcid.org/0000-0001-8621-308X

Twan Lammers − *Institute for Experimental Molecular Imaging, University Hospital Aachen, 52074 Aachen, Germany;* orcid.org/0000-0002-1090-6805

Complete contact information is available at: https://pubs.acs.org/10.1021/acs.bioconjchem.0c00593

Author Contributions

#M.D. and R.H. contributed equally.

Notes

The authors declare no competing financial interest.

■ ACKNOWLEDGMENTS

This research was supported by the Deutsche Forschungsgemeinschaft (DFG) in the framework of the Research Training Group 2375 "Tumor-targeted Drug Delivery" grant 331065168, DFG FOR 2591 to FK Grant No. 321137804 and CRC 10662. The authors gratefully acknowledge Se-Hyeong Jung from DWI − Leibniz-Institute or Interactive Materials for assistance with multiangle DLS measurements.

■ REFERENCES

(1) Bray, F., Ferlay, J., Soerjomataram, I., Siegel, R. L., Torre, L. A., and Jemal, A. (2018) Global Cancer Statistics 2018: GLOBOCAN Estimates of Incidence and Mortality Worldwide for 36 Cancers in 185 Countries. *Ca-Cancer J. Clin. 68* (6), 394−424.

(2) Coates, A., Abraham, S., Kaye, S. B., Sowerbutts, T., Frewin, C., Fox, R. M., and Tattersall, M. H. (1983) On the Receiving End–Patient Perception of the Side-Effects of Cancer Chemotherapy. *Eur. J. Cancer Clin. Oncol. 19* (2), 203−208.

(3) Mukherjee, B. (2014) Nanosize Drug Delivery System. *Curr. Pharm. Biotechnol. 14* (15), 1221.
(4) Golombek, S. K., May, J.-N., Theek, B., Appold, L., Drude, N., Kiessling, F., and Lammers, T. (2018) Tumor Targeting via EPR: Strategies to Enhance Patient Responses. *Adv. Drug Delivery Rev. 130*, 17−38.
(5) Zwicke, G. L., Mansoori, G. A., and Jeffery, C. J. (2012) Utilizing the Folate Receptor for Active Targeting of Cancer Nanotherapeutics. *Nano Rev. 3*, 18496.
(6) Maiti, S., and Paira, P. (2018) Biotin Conjugated Organic Molecules and Proteins for Cancer Therapy: A Review. *Eur. J. Med. Chem. 145*, 206−223.
(7) Sanches, S. C., Ramalho, L. N. Z., Mendes-Braz, M., Terra, V. A., Cecchini, R., Augusto, M. J., and Ramalho, F. S. (2014) Riboflavin (Vitamin B-2) Reduces Hepatocellular Injury Following Liver Ischaemia and Reperfusion in Mice. *Food Chem. Toxicol. 67*, 65−71.
(8) Liu, D., and Zempleni, J. (2014) Low Activity of LSD1 Elicits a Pro-Inflammatory Gene Expression Profile in Riboflavin-Deficient Human T Lymphoma Jurkat Cells. *Genes Nutr. 9* (5), 1 DOI: 10.1007/s12263-014-0422-6.
(9) Yonezawa, A., and Inui, K. (2013) Novel Riboflavin Transporter Family RFVT/SLC52: Identification, Nomenclature, Functional Characterization and Genetic Diseases of RFVT/SLC52. *Mol. Aspects Med. 34* (2), 693−701.
(10) Bareford, L. M., Avaritt, B. R., Ghandehari, H., Nan, A., and Swaan, P. W. (2013) Riboflavin-Targeted Polymer Conjugates for Breast Tumor Delivery. *Pharm. Res. 30* (7), 1799−1812.
(11) Bareford, L. M., Phelps, M. A., Foraker, A. B., and Swaan, P. W. (2008) Intracellular Processing of Riboflavin in Human Breast Cancer Cells. *Mol. Pharmaceutics 5* (5), 839−848.
(12) Karande, A. A., Sridhar, L., Gopinath, K. S., and Adiga, P. R. (2001) Riboflavin Carrier Protein: A Serum and Tissue Marker for Breast Carcinoma. *Int. J. Cancer 95* (5), 277−281.
(13) Rao, P. N., Levine, E., Myers, M. O., Prakash, V., Watson, J., Stolier, A., Kopicko, J. J., Kissinger, P., Raj, S. G., and Raj, M. H. G. (1999) Elevation of Serum Riboflavin Carrier Protein in Breast Cancer. *Cancer Epidemiol. Biomarkers Prev. 8*, 985−990.
(14) Bartmann, L., Schumacher, D., Von Stillfried, S., Sternkopf, M., Alampour-Rajabi, S., van Zandvoort, M., Kiessling, F., and Wu, Z. (2019) Evaluation of Riboflavin Transporters as Targets for Drug Delivery and Theranostics. *Front. Pharmacol. 10*, 1 DOI: 10.3389/fphar.2019.00079.
(15) Johnson, T. M., Ouhtit, A., Gaur, R., Fernando, A., Schwarzenberger, P. O., Su, J. L., Ismail, M. F., El-Sayyad, H. I. H., Karande, A., Elmageed, Z. Y. A., et al. (2009) Biochemical Characterization of Riboflavin Carrier Protein (RCP) in Prostate Cancer. *Front. Biosci., Landmark Ed. 14*, 3634−3640.
(16) Rao, P. N., Crippin, J., Levine, E., Hunt, J., Baliga, S., Balart, L., Anthony, L., Mulekar, M., and Raj, M. H. G. (2006) Elevation of Serum Riboflavin Carrier Protein in Hepatocellular Carcinoma. *Hepatol. Res. 35* (2), 83−87.
(17) Jiang, X.-R., Yu, X.-Y., Fan, J.-H., Guo, L., Zhu, C., Jiang, W., and Lu, S.-H. (2014) RFT2 Is Overexpressed in Esophageal Squamous Cell Carcinoma and Promotes Tumorigenesis by Sustaining Cell Proliferation and Protecting against Cell Death. *Cancer Lett. 353* (1), 78−86.
(18) Long, L., Pang, X.-X., Lei, F., Zhang, J.-S., Wang, W., Liao, L.-D., Xu, X.-E., He, J.-Z., Wu, J.-Y., Wu, Z.-Y., et al. (2018) SLC52A3 Expression Is Activated by NF-KB P65/Rel-B and Serves as a Prognostic Biomarker in Esophageal Cancer. *Cell. Mol. Life Sci. 75* (14), 2643−2661.
(19) Fu, T., Liu, Y., Wang, Q., Sun, Z., Di, H., Fan, W., Liu, M., and Wang, J. (2016) Overexpression of Riboflavin Transporter 2 Contributes toward Progression and Invasion of Glioma. *NeuroReport 27* (15), 1167−1173.
(20) Darguzyte, M., Drude, N., Lammers, T., and Kiessling, F. (2020) Riboflavin-Targeted Drug Delivery. *Cancers 12* (2), 295.
(21) Ostuni, E., Chapman, R. G., Holmlin, R. E., Takayama, S., and Whitesides, G. M. (2001) A Survey of Structure−Property Relationships of Surfaces That Resist the Adsorption of Protein. *Langmuir 17* (18), 5605−5620.
(22) Lau, K. H. A., Ren, C., Sileika, T. S., Park, S. H., Szleifer, I. G., and Messersmith, P. B. (2012) Surface-Grafted Polysarcosine as a Peptoid Antifouling Polymer Brush. *Langmuir 28* (46), 16099−16107.
(23) Barz, M., Luxenhofer, R., Zentel, R., and Vicent, M. J. (2011) Overcoming the PEG-Addiction: Well-Defined Alternatives to PEG, from Structure−Property Relationships to Better Defined Therapeutics. *Polym. Chem. 2* (9), 1900−1918.
(24) Huesmann, D., Sevenich, A., Weber, B., and Barz, M. (2015) A Head-to-Head Comparison of Poly(Sarcosine) and Poly(Ethylene Glycol) in Peptidic, Amphiphilic Block Copolymers. *Polymer 67*, 240−248.
(25) Holm, R., Douverne, M., Weber, B., Bauer, T., Best, A., Ahlers, P., Koynov, K., Besenius, P., and Barz, M. (2019) Impact of Branching on the Solution Behavior and Serum Stability of Starlike Block Copolymers. *Biomacromolecules 20* (1), 375−388.
(26) Holm, R., Weber, B., Heller, P., Klinker, K., Westmeier, D., Docter, D., Stauber, R. H., and Barz, M. (2017) Synthesis and Characterization of Stimuli-Responsive Star-Like Polypept(o)Ides: Introducing Biodegradable PeptoStars. *Macromol. Biosci. 17* (6), 1600514.
(27) Holm, R., Schwiertz, D., Weber, B., Schultze, J., Kuhn, J., Koynov, K., Lächelt, U., and Barz, M. (2020) Multifunctional Cationic PeptoStars as SiRNA Carrier: Influence of Architecture and Histidine Modification on Knockdown Potential. *Macromol. Biosci. 20*, e1900152.
(28) Li, P., Liu, S., Wang, X., Liu, Z., and He, Y. (2013) Fluorescence Quenching Studies on the Interaction of Riboflavin with Tryptophan and Its Analytical Application: Fluorometric Method for the Determination of VB2. *Luminescence 28* (6), 910−914.
(29) Meding, J., Urich, M., Licha, K., Reinhardt, M., Misselwitz, B., Fayad, Z. A., and Weinmann, H.-J. (2007) Magnetic Resonance Imaging of Atherosclerosis by Targeting Extracellular Matrix Deposition with Gadofluorine M. *Contrast Media Mol. Imaging 2* (3), 120−129.
(30) Beztsinna, N., Tsvetkova, Y., Bartneck, M., Lammers, T., Kiessling, F., and Bestel, I. (2016) Amphiphilic Phospholipid-Based Riboflavin Derivatives for Tumor Targeting Nanomedicines. *Bioconjugate Chem. 27* (9), 2048−2061.
(31) Tsvetkova, Y., Beztsinna, N., Baues, M., Klein, D., Rix, A., Golombek, S. K., Al Rawashdeh, W., Gremse, F., Barz, M., Koynov, K., et al. (2017) Balancing Passive and Active Targeting to Different Tumor Compartments Using Riboflavin-Functionalized Polymeric Nanocarriers. *Nano Lett. 17* (8), 4665−4674.
(32) Miller, M. A., Zheng, Y.-R., Gadde, S., Pfirschke, C., Zope, H., Engblom, C., Kohler, R. H., Iwamoto, Y., Yang, K. S., Askevold, B., et al. (2015) Tumour-Associated Macrophages Act as a Slow-Release Reservoir of Nano-Therapeutic Pt(IV) pro-Drug. *Nat. Commun. 6* (1), 1−13.

https://dx.doi.org/10.1021/acs.bioconjchem.0c00593
Bioconjugate Chem. 2020, 31, 2691−2696